Intercalation pseudocapacitance of expanded graphite in sodium-ion capacitors

Zhendong Zhang, Jiachang Zhao ✉, *Chaofei Guo, Jingli Xu*

College of Chemistry and Chemical Engineering, Shanghai University of Engineering Science, Shanghai 201620, People's Republic of China
✉ *E-mail: zjc@sues.edu.cn*

Published in Micro & Nano Letters; Received on 29th September 2017; Revised on 15th January 2018; Accepted on 26th January 2018

The intercalation pseudocapacitance of expanded graphite (EG) which was prepared by a process of oxidation and partial reduction on pristine graphite was investigated in this work. The structure of EG was characterised by X-ray diffraction (XRD) and high-resolution transmission electron microscope (HRTEM), and the electrochemical performance of EG was measured by cyclic voltammetry, galvanostatic charge–discharge and electrochemical impedance spectroscopy. The interlayer distance of EG is enlarged from 0.34 to 0.40 nm, which is demonstrated by XRD and HRTEM. EG electrode exhibits a specific capacitance of 228 F/g at current density of 0.5 A/g. Moreover, the material shows excellent cycle stability after 2000 charge–discharge cycles at a current density of 1 A/g. EG could be a very promising material for the supercapacitors industry.

1. Introduction: Nowadays, as people pay more attention to energy and environmental problems, non-conventional energy devices such as batteries, fuel cells and supercapacitors have been widely researched throughout the world [1–6]. Electrochemical supercapacitors, which are one of the non-conventional energy devices, have attracted considerable interest because of their high specific capacitance, high-power density and long cycle life [7–9]. Based on the energy storage mechanisms, supercapacitors can be divided into two categories: electrical double layer capacitors and pseudocapacitors [10]. Generally speaking, the latter exhibits much higher specific capacitances than the former.

Intercalation pseudocapacitance, as one of three mechanisms leading to pseudocapacitance, occurs when ions intercalate into interlayer gaps (van der Waals gaps) of layered or tunnel materials accompanied by a faradaic charge transfer with no crystallographic phase change [11, 12]. The relevant materials exhibiting intercalation pseudocapacitance are α-MoO_3 [11], orthorhombic Nb_2O_5 [13], MoS_2 nanosheets [14], exfoliated MoS_2 [12], MoO_{3-x} nanobelt/carbon nanotube films [15], MoO_2 [16]. Although most of these materials are intercalated by Li^+, Na^+ intercalated electrode materials are attracting people's attention due to the natural abundance and low cost of sodium compared with lithium [17, 18].

Expanded graphite (EG) has been used as anode materials for sodium-ion batteries due to its larger interlayer distance compared with graphite that can hardly be intercalated by Na^+ [19, 20]. In this Letter, we report the synthesis and intercalation pseudocapacitance of EG in sodium-ion capacitors.

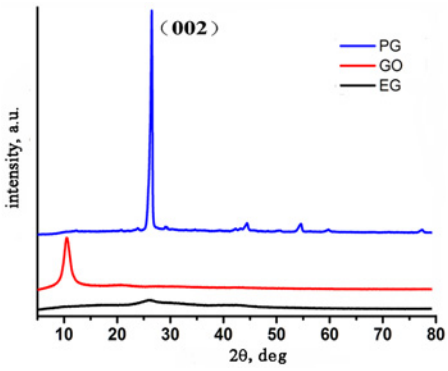

Fig. 1 *XRD patterns of PG, GO and EG*

2. Experimental procedure: Graphite oxide (GO) was prepared from pristine graphite (PG) by using modified Hummer's method as described by Wen *et al.* [19]. EG was synthesised via partial reducing process of GO. In tube furnace GO powder was put into a quartz boat under the protection of nitrogen. The temperature is raised from 20 to 600°C with a heating rate of 5 °C/min and kept for 1 h, and allowed to cool to ambient temperature. After that this simple was collected.

Powder X-ray diffraction (XRD) patterns were recorded on a Bruker D8 Advance diffractometer with CuKα radiation ($\lambda = 0.15406$ nm). High-resolution transmission electron microscope (HRTEM) was carried out with a JEOL 2010 microscope. The electrode was formed by mixing EG or PG, ketjen black and PTFE as binder with a mass ratio of 85:10:5 on a thin sheet of foamed nickel, and the electrochemical measurements were performed in a three-electrode system on a computerised potentiostat (CHI660C electrochemical workstation), in which EG or PG was used as the working electrode; a platinum foil and an Hg/HgO

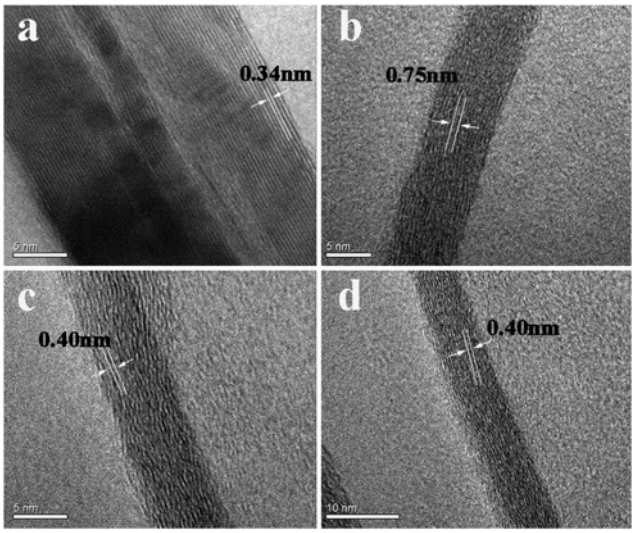

Fig. 2 *HRTEM images of*
a PG
b GO
c, *d* EG

were used as the counter and reference electrodes, respectively. 2 M NaOH was used as the electrolyte. The electrochemical measurements include cyclic voltammetry (CV), galvanostatic current charge discharge and electrochemical impedance spectroscopy (EIS). The specific capacitance of the electrode materials was calculated from the charge–discharge curves using :

$$C = \frac{It}{m\Delta V} \tag{1}$$

where I, t, m and ΔV are applied current, discharge time, active mass and voltage, respectively.

3. Results and discussion: In order to analyse the crystal structure, the three samples of PG, GO and EG were characterised by XRD and the XRD patterns are shown in Fig. 1. The XRD pattern of PG exhibits a sharp peak at $2\theta = 26.4°$, corresponding to the (002) crystal planes of the typical graphite layer with an interlayer distance of 0.34 nm. After oxidation, the peak of GO shifts to $2\theta = 11.5°$, suggesting an enlarged interlayer distance. This is because the intercalation of oxygen-containing groups attached to two sides of the single graphene plane, causing distortion of the interlayer structure. The diffraction peak of EG turns back to $2\theta = 25.1°$, which is smaller than that of PG, exhibiting a graphite-like structure with a larger interlayer distance.

In order to investigate the microstructure of the samples, further structural analyses were conducted by using HRTEM. As depicted in Fig. 2*a*, long-range ordered lattices were clearly observed in the PG. The distances between the two adjacent lattice planes are measured to be 0.34 nm. In Fig. 2*b*, long-range order is interrupted by tremendous insertion of oxygen in the graphite interlayer after oxidation, leaving a pattern with only localised short-range ordering, and the observed fringe spacing of GO is 0.75 nm. After thermal reduction, as shown in Figs. 2*c* and *d*, EG tends to long-range order morphology, which is much easier for intercalation of sodium ion. Moreover, the interlayer distance is significantly boosted from 0.34 to 0.40 nm. Obviously, the distance between PG layers is expanded after the oxidation reactions due to the insertion of oxygen-containing groups.

From the XRD and HRTEM patterns, it becomes apparent that the graphite was expanded, and the interlayer distance is enlarged from 0.34 to 0.40 nm

The capacitive performances of EG were demonstrated by CV tests. The CV measurement has been carried out using various scan rates in the voltage range of −1 to 0 V at room temperature in 2.0 M NaOH electrolyte, as shown in Fig. 3*a*. These CV patterns

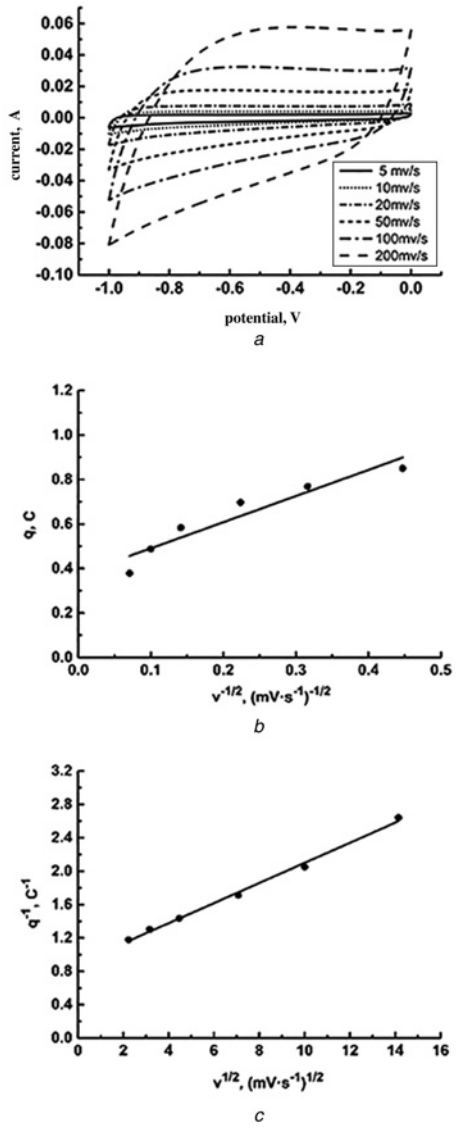

Fig. 3 *Capacitive performances of EG*
a CVs of EG electrode at the different sweep rates
b Extrapolation of q to $v = \infty$ from the q versus $v^{-1/2}$ plot given the outer charge
c Extrapolation of q to $v = 0$ from the q^{-1} versus $v^{1/2}$ plot given the total charge for EG

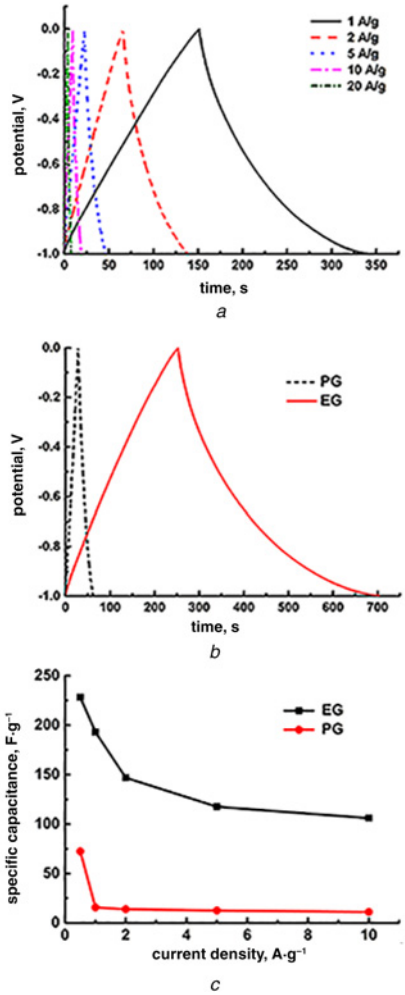

Fig. 4 *Capacitive performances of EG and PG*
a GCD profiles of EG
b GCD profiles of EG anf PG
c Specific capacitance of EG anf PG

doi: 10.1049/mnl.2017.0714

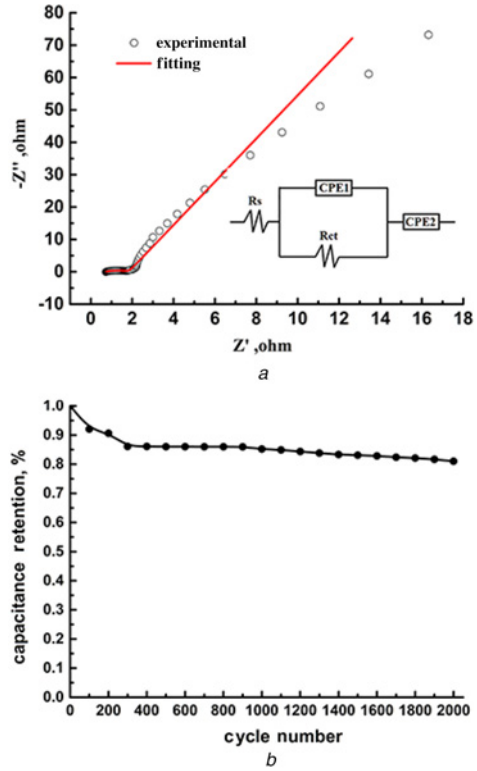

Fig. 5 *Electrochemical performances of EG*
a Nyquist plot and fitting curve for EG electrode
b Cycling stability of EG electrode

show a nearly rectangular mirror-image current response on voltage reversal without obvious redox peaks. Remarkably, the semi-rectangular shape of CV curve for EG electrode is maintained at the high scan rate of 200 mV/s, indicating the good capacitance behaviour and low contact resistance.

In order to investigate the charge and discharge mechanism of EG, the functions between voltammetric charges (q) and scan rate have been erected. The dependences of q on $v^{-1/2}$ and q^{-1} on $v^{1/2}$ are shown in Fig. 3. At a high scan rate, the electrochemical response depends only on the outer active surface due to the slow intercalation of Na^+ into the lattice of EG caused by diffusion limitation. The extrapolation of q to $v=\infty$ from the q versus $v^{-1/2}$ plot (Fig. 3*b*) gives the outer charge (q_0), which is related to the outer and more accessible active surface. At a low scan rate, Na+ has enough time to diffuse into the lattice of EG. The extrapolation of q to $v=0$ from the q^{-1} versus $v^{1/2}$ (Fig. 3*c*) gives the total charge (q_T) [21, 22]. q_T and q_0 are 0.560 and 0.187 C, respectively, and the percentage of outer charge is 33.4%, suggesting that the charge storage mechanism is mainly based on intercalation pseudocapacitance.

Further research about the reliable capacitive performance of EG electrode is investigated. Fig. 4*a* shows the galvanostatic charge–discharge (GCD) curves of the EG electrode tested at different current densities from 1 to 20 A/g. The triangular charge–discharge characteristics are systematically increased, suggesting that the supercapacitor based on EG has good electrochemical reversibility and charge-discharge performances. From Fig. 4*b*, the contrast of charge–discharge time between EG with PG is clearly provided, and charge–discharge time of the former is higher than the latter. An even more striking comparison is from Fig. 4*c*. The discharge capacitances of EG and PG were calculated and plotted as a function of current density. The EG electrode delivers very large capacitances of 228, 193, 146.8, 117.5, 106 and 108 F/g at current densities of 0.5, 1, 2, 5 and 10 A/g, respectively. By comparison, PG electrode shows low capacitances of 72.4, 15.6, 13.8, 12.5 and 11.0 F/g at current densities of 0.5, 1, 2, 5 and 10 A/g, respectively. The specific capacitance of EG is higher than that of activated carbons as previously reported by other groups [23, 24].

Fig. 5*a* represents the EIS spectrum of EG electrode in the frequency ranging from 0.01 to 5000 Hz and its equivalent circuit according to ZSimpWin software. The results show that R_s, which represents electrolyte resistance, is 0.728 Ω. Meanwhile, charge transport resistance (R_{ct}) is only 1.105 Ω. The low value of R_{ct} is desired for high-power density of supercapacitors. The exponent of CPE2 is 0.905, indicating the remarkable intercalation pseudocapacitance. Hence, EIS results suggest EG as a good alternative for high-performance supercapacitor application. The long-term electrochemical stability of EG electrode was tested by repeated GCD cycling about 2000 cycles at a current density of 1 A/g. Fig. 5*b* clearly illustrates that the EG electrode possesses capacitance retention of about 81.06% even after 2000 cycles.

4. Conclusion: In this Letter, EG was prepared by a process of oxidation and partial reduction on PG. The results of XRD and HRTEM show that the interlayer distance of EG is enlarged from 0.34 to 0.40 nm. The EG electrode exhibits a specific capacitance of 228 F/g at 0.5 A/g in three electrode system. Furthermore, the material shows excellent cycle stability after 2000 charge–discharge cycles at a current density of 1 A/g. EG is a promising candidate for application in sodium-ion capacitors.

5. Acknowledgment: This work was supported by National Natural Science Foundation of China (grant no. 51602193).

6 References

[1] Bonaccorso F., Colombo L., Yu G., *ET AL.*: 'Graphene, related two-dimensional crystals, and hybrid systems for energy conversion and storage', *Science*, 2015, **347**, p. 1246501
[2] Peng L., Zhu Y., Chen D., *ET AL.*: 'Two-dimensional materials for beyond-lithium-ion batteries', *Adv. Energy Mater.*, 2016, **6**, p. 1600025
[3] Yan C., Lv C., Zhu Y., *ET AL.*: 'Engineering 2D nanofluidic Li-ion transport channels for superior electrochemical energy storage', *Adv. Mater.*, 2017, **29**, p. 46
[4] Peng L., Zhu Y., Peng X., *ET AL.*: 'Effective interlayer engineering of two-dimensional $VOPO_4$ nanosheets via controlled organic intercalation for improving alkali ion storage', *Nano Lett..*, 2017, **17**, pp. 6273–6279
[5] Yan C., Zhu Y., Li Y., *ET AL.*: 'Local built-in electric field enabled in carbon-doped Co_3O_4 nanocrystals for superior lithium-ion storage', *Adv. Funct. Mater.*, 2018, doi: 10.1002/adfm.201705951
[6] Zhu Y., Peng L., Chen D., *ET AL.*: 'Intercalation pseudocapacitance in ultrathin $VOPO_4$ nanosheets: toward high-rate alkali-ion-based electrochemical energy storage', *Nano Lett..*, 2015, **16**, pp. 742–747
[7] Tang Y.F., Liu Y.Y., Yu S.G., *ET AL.*: 'Comparative study on three commercial carbons for supercapacitor applications', *Russ. J. Electrochem.*, 2015, **5**, pp. 77–78
[8] Wang T.L., Wang W., Dai Y.T., *ET AL.*: 'Electrochemical synthesis of polyaniline films on activated carbon for supercapacitor application', *Russ. J. Electrochem.*, 2015, **51**, p. 743
[9] Wang X.W., Wu K.L., Zhang Z.X., *ET AL.*: 'Synthesis of Ni-riched NiO-Co_3O_4 sheet-like nanocomposites and their application in supercapacitors', *Micro Nano Lett..*, 2015, **10**, pp. 9–11
[10] Li J.F., Zan G.T., Wu Q.S., *ET AL.*: 'An ultra-high-performance anode material for supercapacitors: self-assembled long Co_3O_4 hollow tube network with multiple heteroatom (C-, N- and S-) doping', *J. Mater. Chem. A*, 2016, **4**, p. 9097
[11] Torsten B., Wang J., H S., *ET AL.*: 'Ordered mesoporous α-MoO_3 with iso-oriented nanocrystalline walls for thin-film pseudocapacitors', *Nature Mater.*, 2010, **9**, p. 146
[12] Yoo H.D., Li Y.F., Liang Y.L., *ET AL.*: 'Intercalation pseudocapacitance of exfoliated molybdenum disulfide for ultrafast energy storage', *Chemnanomat*, 2016, **2**, pp. 688–691
[13] Augustyn V., Come J., Michael A.L., *ET AL.*: 'High-rate electrochemical energy storage through Li^+ intercalation pseudocapacitance', *Nature Mater.*, 2013, **12**, p. 518

[14] Acerce M., Damien V., Manish C., *ET AL.*: 'Metallic 1T phase MoS_2 nanosheets as supercapacitor electrode materials', *Nat. Nanotechnol.*, 2015, **10**, pp. 313–318
[15] Xiao X., Peng Z.H., Chen C., *ET AL.*: 'Freestanding MoO_3-x nanobelt/carbon nanotube films for Li-ion intercalation pseudocapacitors', *Nano Energy*, 2014, **9**, pp. 355–363
[16] Li X.Y., Shao J., Li J., *ET AL.*: 'Ordered mesoporous MoO_2 as a high-performance anode material for aqueous supercapacitors', *J. Power Sources*, 2013, **237**, pp. 80–83
[17] Chen C., Wen Y.W., Hu X.L., *ET AL.*: 'Na^+ intercalation pseudocapacitance in graphene-coupled titanium oxide enabling ultra-fast sodium storage and long-term cycling', *Nat. Commun.*, 2015, **6**, p. 6929
[18] Gao S., Zhao J.C., Zhao Y., *ET AL.*: 'Na_2cosio_4 as a novel positive electrode material for sodium-ion capacitors', *Mater. Lett*, 2014, **158**, pp. 300–303
[19] Wen Y., He K., Zhu Y.J., *ET AL.*: 'Expanded graphite as superior anode for sodium-ion batteries', *Nat. Commun*, 2015, **5**, p. 4033
[20] Ramos A., Cameán I., Cuesta N., *ET AL.*: 'Expanded graphitic materials prepared from micro- and nanometric precursors as anodes for sodium-ion batteries', *Electrochim. Acta*, 2016, **187**, pp. 496–507
[21] Jun Y., Zhuang J.F.: 'Carbon nanotube/MnO_2 composites synthesized by microwave-assisted method for supercapacitors with high power and energy densities', *J. Power Sources*, 2009, **194**, pp. 1202–1207
[22] Xu C.J., Bao H., Li H.D., *ET AL.*: 'Electrochemical properties of nanosized hydrous manganese dioxide synthesized by a self-reacting microemulsion method', *J. Power Sources*, 2008, **180**, pp. 664–670
[23] Wu M.B., *ET AL.*: 'Synthesis of starch-derived mesoporous carbon for electric double layer capacitor', *Chem. Eng. J.*, 2014, **245**, pp. 166–172
[24] Zhao Z.H., Liu M.X., Chen L.W., *ET AL.*: 'Ultramicroporous carbon nanoparticles for the high-performance electrical double-layer capacitor electrode', *Energy Fuels*, 2014, **28**, pp. 1561–1568

doi: 10.1049/mnl.2017.0714